Physical Processes of Tableting

E. N. HIESTAND ˣ, J. E. WELLS, C. B. PEOT, and J. F. OCHS

Abstract □ Shear deformation was shown to occur during the decompression of large compacts made by nonisostatic compression. Some materials undergo fracture when these shear stresses are developed. Other materials withstand these stresses but fracture upon ejection when the stress concentrations at the edge of the die are large. Failure to fracture seems to be related to the ability to relieve stresses by plastic deformation. A test was devised to measure this property, called the brittle fracture propensity.

Keyphrases □ Tablet formation—fracture caused by shear stresses during decompression, effect of plastic deformation □ Dosage forms—tablets, fracture caused by shear stresses during decompression, effect of plastic deformation □ Plastic deformation—effect on tablet fracture caused by shear stresses during decompression

It is generally accepted that compact formation by pressure occurs because of forces acting at the areas of true interparticle contact. However, the failure to obtain an intact compact from the compression–decompression cycle is a bit more mysterious. A series of arguments and some supporting evidence indicate that the stresses induced by elastic rebound and the associated deformation processes during decompression are principally responsible for the success or failure of compact formation. This report presents experimental results obtained by using several, sometimes complementary procedures. These data support the shift of emphasis to the decompression process.

To present a coherent, conceptual thesis, the discussion of each individual experimental procedure is not comprehensive. Instead, the emphasis is on the contribution of the results to the total concept. Bits are taken from various on-going research investigations. Cumulatively, these studies, even though incomplete, contribute much to the evidence.

Under high compression pressures, the powder particles in a compact are forced into intimate contact, and extensive areas of true contact between particles are formed. Because the magnitude of van der Waals forces across these interfaces is adequate to provide strong bonds, one might expect all materials to form strong, intact compacts after being subjected to compression. However, if too much energy is stored elastically when under compression, the elastic recovery during decompression may break most of these bonds and a soft, crumbly compact will be formed. Excipients are added to most pharmaceutical formulations to compensate for inherent, undesirable properties of the medicament. For example, it is possible to eliminate the storage of excess elastic energy during compression by mixing a plastic excipient with the harder "elastic" material. The plastic material will permanently deform and establish large, true contact areas with the harder material and will do so at relatively low pressures. Thus, during recovery, the stored elastic energy will be inadequate to separate extensive areas of contact, and strong bonding will result.

Even though these statements are reasonable explanations of many observations, every tablet formulator knows that they are inadequate. Often a laminated compact is produced. The individual pieces are dense, strongly bonded fragments. Therefore, sufficient areas of true contact must form during compression; in general, these areas are not destroyed during the elastic recovery, even though those in the fracture plane are destroyed. Thus, the mechanism of fracture is different from that of the formation of a crumbly tablet. Both are believed to result from inadequate plastic flow. A much more detailed look at compression and decompression is necessary to explain the compaction properties of materials and the fracture phenomenon.

EXPERIMENTAL

Tablet Compression—Many of the tablets used were made in a hand press. A square die was used. The cross section of the faces of the punches was 38.1 mm on a side. The tablet compression force was applied by placing the assembly, with punches in place, into an 18-metric ton hydraulic press[1]. The hand press could be pumped manually or by a motor-driven external cylinder to obtain the desired compression force. Both the punch and die had inserts containing diaphram-type strain gauges on the end of a screw[2]. One gauge was flush with the face of the die, and the other gauge was flush with the face of the punch and centered in it.

In one mode of operation, the output from the gauges was coupled at the y-input of an x–y recorder through a switching circuit that converts the recorder into a two-channel input on the y-axis. Calibration was made by placing a square rubber plug into the die and compressing it with known force. At low pressures, a rubber bag filled with water was used in a similar manner.

The known total force on the punches was obtained from a load cell[3] mounted on the press. The load cell was calibrated by applying a dead weight to check the supplier's calibration. Its output could be coupled to the x-input of the x–y recorder. Thus, it was possible to record simultaneously the total applied force, a local punch face pressure, and a local die wall pressure throughout the entire compression–decompression cycle.

An alternative mode of operation was to monitor the output of the load cell on a voltmeter[4] and to couple the die wall gauge to the y-axis and the punch gauge to the x-axis of the recorder.

In addition to the plain punch and an instrumented one, a special punch was made which contained at its center a spring-loaded, retractable pin 1.09 mm in diameter. This punch was used to form the tablet with a center hole to be used in the brittle fracture propensity determination.

The rotary tableting machine used in the lamination study was an instrumented (1) 16-station press[5]. A direct compaction formulation[6], selected to produce desired levels of lamination, was used. Dies and punches (extra deep cup 12.7 mm diameter) were used in the major study. Flat punches were used only to demonstrate the effect of punch shape. To obtain the data on fracture conditions, the precompression force and speeds were selected arbitrarily, with the final compression increased stepwise until lamination or capping occurred.

Tensile Strength—The tensile strength measurements were made by the transverse compression of square compacts. The procedure and apparatus were described previously (2). Since the hydraulic pressure

[1] Model 341-20, Loomis Engineering and Manufacturing Co., Caldwell, N.J.
[2] Model EPS-1228S (die wall) and model EPS-2528-1800 (punch), Entran Devices Inc., Little Falls, N.J.
[3] Model 1221-AF load cell, Interface Inc., Scottsdale, Ariz.
[4] Model 160B digital multimeter, Keithley Instruments, Cleveland, Ohio.
[5] Manesty Betapress, Manesty Machines, Ltd., Liverpool L24 9LQ, England.
[6] With the cupped punches, each tablet contained 150 mg of phenacetin (bolted), 325 mg of microcrystalline cellulose (Avicel 102), 2 mg of colloidal silicon dioxide (Cab-O-Sil), 167 mg of lactose (bolted), and 6 mg of magnesium stearate. With the flat punches, each tablet contained 150 mg of phenacetin (bolted), 221 mg of spray-dried lactose, and 39 mg of magnesium stearate.

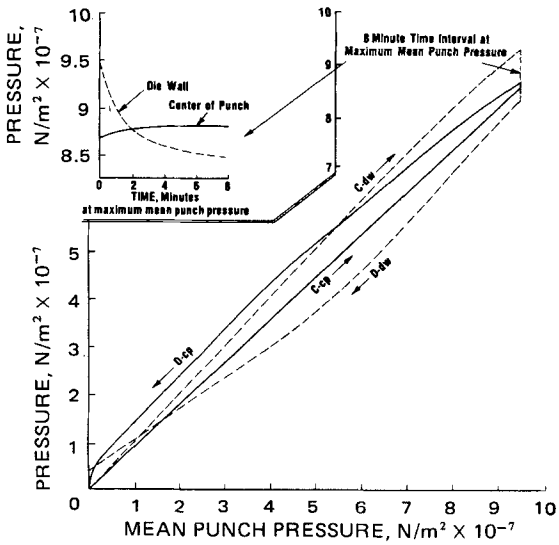

Figure 1—*Sitosterols: change of pressures at die wall and center of punch with average punch pressure during a compression–decompression cycle with a time delay at maximum pressure. Key (dashed lines): C-dw, die wall during compression; and D-dw, die wall during decompression. Key (solid lines): C-cp, center of punch during compression; and D-cp, center of punch during decompression. Insert graph shows changes with time while at maximum compression force.*

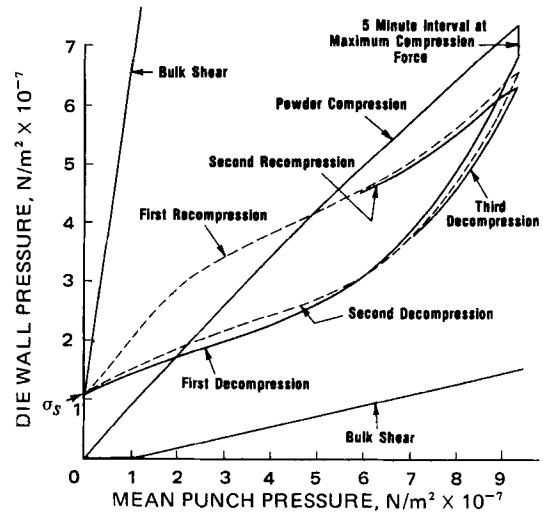

Figure 2—*Die wall* versus *average punch pressure for some compression–recompression cycles of the same sucrose compact. Constant maximum pressure was held on the punch for 5 min before the first decompression. Note that each successive recompression led to a lower maximum die wall pressure. Bulk shear lines were estimated from the uniaxial compression test, which gave* $\alpha = 67°$; σ_s *is failure stress under uniaxial compression.*

in the jack was developed by compression from an external motor-driven cylinder whose speed could be selected, the rate of stress application was controlled. This rate was not critical in experiments exploring this factor. Nevertheless, it is desirable to use a standard rate so that any time-dependent effects are reproduced, should they become important. Even though the external cylinder was driven at a constant rate, the rate of increase of force approximates an exponential curve. In the work reported herein, the rate was selected so that the time between $1/e$ of maximum force to the maximum force was 15 sec.

This apparatus also was used to determine the uniaxial compressive force required to cause a compact to shear. A 38.1-mm square compact was cut into two pieces. One-half was placed in the press with the long axis vertical. The platens covered the entire end of the compact. Blotter material was used on the platen as a pad.

A ring strain-gauge system was used to supply input to a chart recorder to observe the force at fracture. The area of the compact under the platen was calculated from measured dimensions obtained with a micrometer.

Stress Relaxation—The apparatus used by Milosovich was used in the form described by Shlanta and Milosovich (3). One addition was made—*viz.*, an oscilloscope[7] to the output. This oscilloscope permitted one to record photographically the transducer output for the first few seconds of the experiment. The output for the remaining time was recorded on a strip-chart recorder. A 12.7-mm diameter die was used in the studies done in air. The vacuum die was 13 mm in diameter. Powder weights were adjusted to give the same tablet thickness in the two dies.

Another procedure for observing stress relaxation was performed with the hand press, using the instrumented die and punch described previously. This apparatus is flexible, and various procedures may be used. In the work reported in Fig. 1, while the total force on the punch was held constant, the x–y recorder monitored the output of the strain gauges in the punch and die wall. Local pressure changes were observed at the center of the punch face while the mean pressure remained constant. With sucrose (Fig. 2), the punch gauge was not used (due to gauge failure), but the relaxation of the die wall pressure was followed. The load cell on the press indicated the total force on the punch.

Indentation Hardness—The indentation hardness values were measured using the dynamic impact method described previously (4). The chordal radius of the dent was measured with a low powered microscope. The initial and rebound heights were calculated from the arc of the pendulum movement. The indenter was a 25.4-mm diameter steel ball suspended on a 1-m long steel wire (to form the pendulum).

[7] Model B, type 202-1, Tektronix Inc., Portland, Ore.

RESULTS AND DISCUSSION

Compression—The nonisostatic compression of a powdered or granular material to produce a compact is not a simple process. The complexity arises from the numerous simultaneous internal processes that lead to consolidation and bonding. These events include particle rearrangement (consolidation), fracture, and plastic deformation. At the start of the compression, the first dominates; at the end of the compression, the third dominates. In some cases, a fourth phenomenon occurs (5, 6)—*viz.*, localized melting at the interparticle contact points. This phenomenon is believed to be important only with relatively low melting materials. Even very hard asperities are pushed into a more plastic substrate. Thus, the stresses that could produce melting of an asperity are limited by particle hardness. Particle fracture occurs when the stresses within the particles become large enough for a crack to propagate. With some materials, the particles need not fracture because the stresses are relieved by plastic deformation of the particle before their magnitude is sufficient to initiate fracture.

Except in the case of localized asperity melting, the effective area of true contact in a cross-sectional area normal to the direction of pressure application is determined by the product of the force across the plane divided by the permanent deformation pressure of the solid. For simplicity, assume that only one material is present. If the deformation pressure is a constant, then:

$$F = PA \qquad \text{(Eq. 1)}$$

where F is the applied force, P is the permanent deformation pressure of the solid, and A is the effective true contact area in the normal plane.

Therefore, under pressure, a desired maximum true contact area can be established simply by applying adequate pressure. Equation 1 gives no information about the true contact area after elastic recovery; therefore, it is not adequate to predict final compact strength.

By making some general assumptions about the maximum interatomic separation distances that permit significant contributions to bond strength and then applying the Hertz elastic contact relationships (7), it can be deduced that smaller particles should yield larger true contact areas and, thereby, stronger bond strengths. However, the results are not independent of the particle permanent deformation pressures, *i.e.*, their hardness, and hardness may vary with particle size. Furthermore, plastic deformation tends to increase the number of dislocations in a crystal; a hard crystal may first become softer and, if sufficiently "worked," may then become hard again. Thus, the magnitude of P in Eq. 1 usually is unknown. Also, particle size and shape changes may influence the packing density. Thus, speculations on the effect of particle size on tablet bond strength are at best precarious.

Theoretical approaches that use models for the summation of contact areas and forces over a cross-sectional area to obtain true contact areas

are interesting (8, 9) but have not found significant application for solving real problems. Usually, the results deviate only slightly from a linear relationship between true area and force. Unfortunately, the proportionality constant is not known; it is known that the extent of the plastic deformation influences the magnitude of the proportionality constant. Thus, P is an important parameter influencing bond strength.

A more complete description of compaction must include the effects of interparticle friction and friction with the die wall and punches. These contribute to variations of the degree of packing in the die and, therefore, cause a nonuniform density compact to be formed. The variations of density within a compact were reported by Train (10). Furthermore, the effect of die wall friction on pressure at various levels in a compact was studied and described by (11):

$$P_b = P_a \exp\left(-\frac{4L\mu\eta}{D}\right) \qquad \text{(Eq. 2)}$$

where P_a is the applied pressure (punch), P_b is the transmitted pressure at L distance from the punch, D is the diameter, μ is the coefficient of friction, and η is the ratio of radial to axial stress in the compact.

Compression involving movement of both upper and lower punches significantly reduces the density variation within a compact; however, this fact does not eliminate the problem completely. Also, the use of a lubricant and glidant to reduce both interparticle friction and friction with the surfaces of the punch and die contribute significantly to the formation of a more homogeneous compact. Usually, these agents cause an increase in the die wall pressure for a given punch pressure (12), probably because the particles compact more tightly before plastic deformation becomes the dominant consolidation process. Possibly, interparticle "wedging" occurs more easily when friction is reduced and, thereby, increases the die wall pressure.

Thus, several factors may influence the structure of a compact and the magnitude of the die wall pressure at the maximum compression force. It is not easy to establish the relative importance of each. However, a valid qualitative generalization is that when either powders or granules are compressed into a compact, regions of different relative density are produced and the die wall pressure is of higher magnitude than would result from the elastic deformation of a single piece of an isotropic solid. During decompression, this extra die wall pressure may lead to excessively large shear stresses in the compact.

It is instructive to think of plastic deformation both as a change in particle shape and as the sliding of groups of particles within the compact. This approach provides a more macroscopic perspective and is used to explain the redistribution of stresses when under compression. For example, when sitosterols were held under constant compressional force (the total punch force held constant), a localized die wall pressure decreased as a function of time and the pressure at the center of the punch increased simultaneously (Fig. 1, insert graph, which was obtained with the instrumented 38.1-mm square punch and die set). Apparently, at maximum compression, some points in the compact were stressed to the limit of their strength. Since their instantaneous or dynamic shear strength exceeded their static shear strength, internal plastic flow occurred over time to relieve some stress[8]. The center of the punch always is a lower pressure region (10), so the flow was toward the center. Thus, regional density changes occurred and the compact density became slightly less heterogeneous as a result of this macroscopic plastic flow. The rate of the process decreased sharply; thus, a totally uniform density compact did not result.

In Fig. 1, the pressures reported were local pressures known at only two small regions because the strain gauges were less than 6.35 mm in diameter; the compact was a 38.1-mm square. In the absence of better data, it is expedient to use these pressures as very rough estimates of the principal stresses for an assumed isotropic homogeneous compact. In this case, the shear stress is given by:

$$\tau = \frac{\sigma_a - \sigma_r}{2} \sin 2\alpha \qquad \text{(Eq. 3)}$$

where τ is the shear stress at angle α from the direction of the minor principal stress, σ_a is the axial or punch pressure, and σ_r is the radial or die wall pressure.

Whenever τ just exceeds the shear strength of the material, shear failure occurs. If the failure does not cause a fracture plane to develop, the failure is by plastic flow. Obviously, τ has its largest value when $\alpha = 45°$. The shear strength also is a function of the angle α; therefore, the shear strength may be exceeded at some angle greater than 45° before

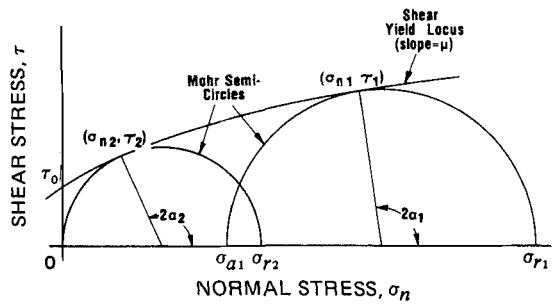

Figure 3—*Shear yield conditions based on the use of a geometric representation of stress analysis equations, a Mohr diagram. Semicircle on right (subscript 1) represents the higher pressure case when the radial pressure is less than the axial pressure. Semicircle on left (subscript 2) represents case when the axial pressure is zero and the residual die wall pressure is* σ_{r2} *(*σ_{r0} *in Eq. 6); it also could describe the uniaxial compression case. In Eq. 5, the yield locus is assumed to be a straight line and* μ *is a constant.*

it is exceeded at $\alpha = 45°$. For a Mohr body, the shear strength is assumed to be a nearly linear function of the compressive stress normal to the shear plane. The normal stress, σ_n, is given by:

$$\sigma_n = \frac{\sigma_a + \sigma_r}{2} + \frac{\sigma_a - \sigma_r}{2} \cos 2\alpha \qquad \text{(Eq. 4)}$$

For the Mohr body, the internal friction coefficient, μ, becomes the proportionality constant for calculating the shear strength, τ_f, and for the linear case:

$$\tau_f = \mu\sigma_{nf} + \tau_0 \qquad \text{(Eq. 5)}$$

where σ_{nf} is the magnitude of the normal stress, σ_n, at failure; τ_0 is the shear strength when $\sigma_n = 0$; and μ is the internal friction coefficient and is related to α by $\mu = -\cot 2\alpha$.

Equations 3–5 are useful in providing some insight into shear failure conditions. A standard geometric representation of Eqs. 3–5 is called a Mohr diagram. Because of symmetry, only half of a Mohr diagram is shown in Fig. 3. It should be useful to use Eqs. 3–5 and the Mohr diagram to discuss shear failure in both the compression and decompression of compacts. The graphical representation of shear failure is correct only when the Mohr circle of stress is tangent to the shear failure yield locus.

Decompression—In this discussion, it is assumed that adequate compressional force was applied to produce densification and bonding; *i.e.*, crumbling from lack of adequate compression with plastic deformation will not be considered further. Even though adequate pressure is applied, the compression–decompression cycle may or may not produce an intact compact without fracture lines in it. Success is determined primarily by the internal processes that occur as the compression stresses are removed. These processes include both removal of punch pressure and ejection from the die.

Powder under compression in a cylindrical die is confined in a radial direction until ejected from the die. Therefore, the major dimensional change during decompression is in the axial direction. Of course, the same is true for recompression of the compact if it is recompressed without removal from the die. Equation 6 describes the stresses associated with elastic deformation of an isotropic solid when the strain in the radial direction is zero:

$$\sigma_r - \sigma_{r0} = \frac{\nu}{1 - \nu} \sigma_a \qquad \text{(Eq. 6)}$$

where ν is the Poisson ratio[9], and σ_{r0} is the die wall pressure intercept value.

The residual die wall pressure, σ_{r0}, would be zero if the compression of an isotropic solid is started with a confined, but unstressed, solid body. If only elastic deformation occurred during compression and decompression, σ_{r0} would remain zero. When one starts with a powder, a finite residual die wall pressure is always observed after completion of the compression–decompression cycle. Obviously, if the compact undergoes shear deformation in both recompression and decompression, gross deviations from the elastic case would be expected and Eq. 6 would not be applicable. (Later, it will become obvious that Eq. 6 is not applicable

[8] This viscoelastic flow is believed to result from random thermal fluctuations breaking prestressed bonds.

[9] The Poisson ratio is defined as the transverse expansion per unit dimension of a solid of uniform cross section to its contraction per unit length when subjected to a uniaxial compressive stress (during elastic deformation).

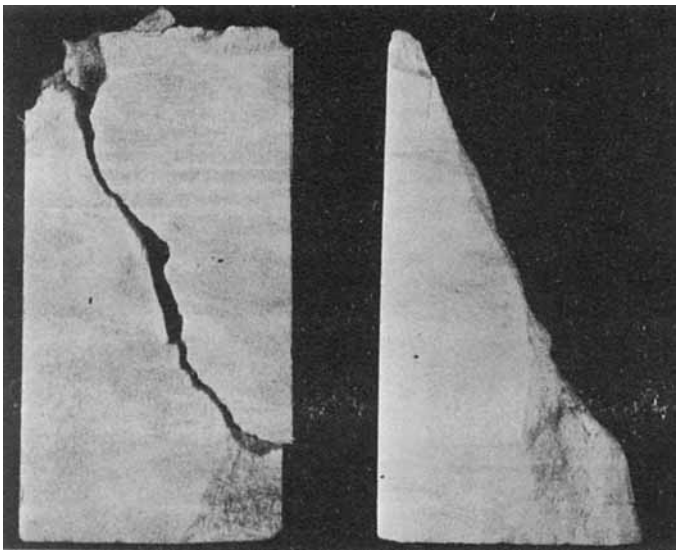

Figure 4—*Sucrose compact fractured in shear under uniaxial compressive stress of 1.1 × 10⁷ N/m². Compact was compressed at 9.2 × 10⁷ N/m². Fracture plane was irregular so value of α was not precise. With various compacts, values ranged from 64 to 67°.*

during the decompression process.) Others (13, 14) considered the possibility of plastic deformation during decompression but approached the subject differently than will be done in the following discussion.

To describe the magnitudes of the die wall and punch pressures that would cause the compact to fail in shear, the following equations are developed. Taking derivatives of Eqs. 3 and 4 with respect to σ_r and combining to obtain $d\tau_f/d\sigma_{rf}$ yield:

$$\frac{d\tau_f}{d\sigma_{nf}} = \frac{\left(\frac{d\sigma_{af}}{d\sigma_{rf}} - 1\right)\sin^2 2\alpha_f + 2(\sigma_{af} - \sigma_{rf})\frac{d\alpha_f}{d\sigma_{rf}}}{\left(\frac{d\sigma_{af}}{d\sigma_{rf}} + 1\right)\cos 2\alpha_f + \left(\frac{d\sigma_{af}}{d\sigma_{rf}} - 1\right)\cos^2 2\alpha_f - 2(\sigma_{af} - \sigma_{rf})\frac{d\alpha_f}{d\sigma_{rf}}} \cot 2\alpha_f \qquad \text{(Eq. 7)}$$

The subscript f was added to indicate a condition of failure.

By definition:

$$\frac{d\tau_f}{d\sigma_{nf}} = \mu = -\cot 2\alpha \qquad \text{(Eq. 8)}$$

Combining Eqs. 7 and 8 gives:

$$\frac{d\sigma_{af}}{d\sigma_{rf}} = \frac{1 - \cos 2\alpha}{1 + \cos 2\alpha} = \frac{\sqrt{1+\mu^2} + 1}{\sqrt{1+\mu^2} - 1} \qquad \text{(Eq. 9)}$$

Equation 9 permits the estimation of the limiting stresses beyond which shear occurs once μ or an equivalent value has been determined. While μ may not be a constant, large variations are not expected as long as only compressive stresses are used.

At least in theory, the uniaxial compression of a compact should provide the necessary data for use of Eq. 9. For this experiment, a large square compact was cut into two equal pieces and a compressive stress was applied along its long axis until it fractured. If both the fracture angle, α, and the compressive stress at fracture can be measured, Eqs. 8 and 9 can be evaluated. Figure 4 shows a sucrose compact fractured under uniaxial stress; the magnitude of the observed fracture stress is plotted on Fig. 2 (point σ_s). The irregular fracture line shown in Fig. 4 makes an accurate evaluation difficult. Compacts of most materials are even less satisfactory because of laminations and other aberrant fracture planes.

The two bulk shear lines in Fig. 2 have slopes calculated by Eq. 9 using the uniaxial compression data. Both α and μ were taken as constants; hence, straight lines are shown. These lines cross the axis at the uniaxial compression stress for fracture. The slopes of the two lines are reciprocals of each other; the distinction between σ_{af} and σ_{rf} in Eq. 9 is artificial; *i.e.*, it does not matter which is larger, only the difference is important. As is obvious in Fig. 2, these lines do not correspond to the experimental range of σ_{rf} *versus* σ_{af}. While this finding suggests that the experimental compression–decompression stresses are within the elastic limits of the material, further examination, such as of the data in Fig. 5, indicates that shear is occurring in the regions between these lines.

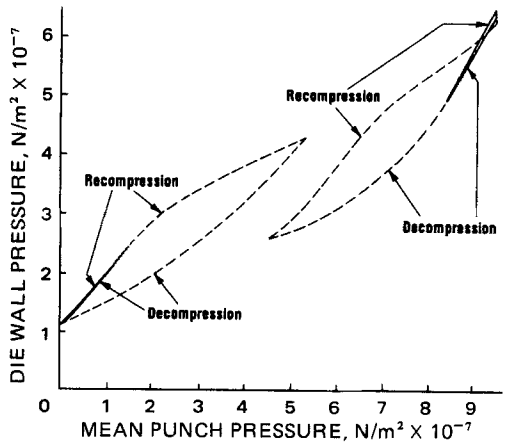

Figure 5—*Sucrose compact compressed as in Fig. 2 but recompression–decompression cycles were partials. Key: solid lines on left, recompression–decompression over very limited range of pressure; dashed lines on left, recompression–decompression cycle extended into decreasing slope region; solid lines on right, decompression–recompression cycle over limited range of pressures but starting from maximum values; and dashed lines on right, decompression–recompression cycle extended into decreasing slope region. Loops are believed to indicate that plastic deformation occurred at local points. Very small loops with solid lines may be due to friction resisting punch movement.*

The uniaxial fracture stress is an estimate of the magnitude of the die wall pressure at failure when the punch pressure is zero and vice versa. Figure 2 shows data for die wall *versus* punch pressures obtained for compression–decompression cycles using sucrose. The die wall pressure is that measured at the center of one side of a square compact. The punch pressure is the mean value based on the total force applied to the punch. When the punch pressure went to zero, the die wall pressure became identical to the uniaxial compressive strength, σ_s. Obviously, the shear strength limited the residual die wall pressure. This value remained essentially constant even after repeated recompression cycles.

The shapes of the decompression plot reported here are very different from those reported by Leigh *et al.* (13) and Carless and Leigh (14). Possibly, the differences arise from differences in the procedure and instrumentation. Those investigators measured total die wall force and not local pressures. Furthermore, the present apparatus is very rigid; *i.e.*, the entire die expands very little under pressure. Other differences are size and shape of compacts and the rate of compression and decompression. When Poisson ratios are calculated from the data reported here, unrealistically large values are obtained. Thus, the data measured at separated regions of the compact surface do not seem to be representative of a single, small volume element. However, the theoretical arguments developed from these data do not depend on the exact shape of the die wall *versus* punch pressure plot.

Upon recompression followed by decompression, as was done to obtain the data in Fig. 2, a "hysteresis" type of loop is formed. If the compression–decompression involves only elastic deformation, the compression–decompression pathway should be identical. Therefore, plastic deformation must be occurring during each recompression–decompression cycle. Partial recompression–decompression cycles are even more revealing (Fig. 5). If the recompression pressure is limited to a value below the first bend, the decompression line from that point superimposes onto the compression line (solid lines on the left of Fig. 5). However, when the recompression pressure is increased to a point beyond the first bend, a loop is formed upon decompression. Apparently, the first portion of the recompression curve represents elastic deformation while larger compression forces introduce plastic deformation.

Results of a similar experiment at the start of the decompression is shown on the right side of Fig. 5. If the decompression from maximum applied force is stopped short of the first bend, recompression from that point retraces essentially the same line. (A slight deviation occurs, possibly due to friction.) Therefore, the first part of the decompression is an elastic deformation. However, if the decompression is stopped at a pressure beyond the first bend, the recompression from that point forms a loop. Therefore, shear or plastic deformation is occurring during much of the decompression.

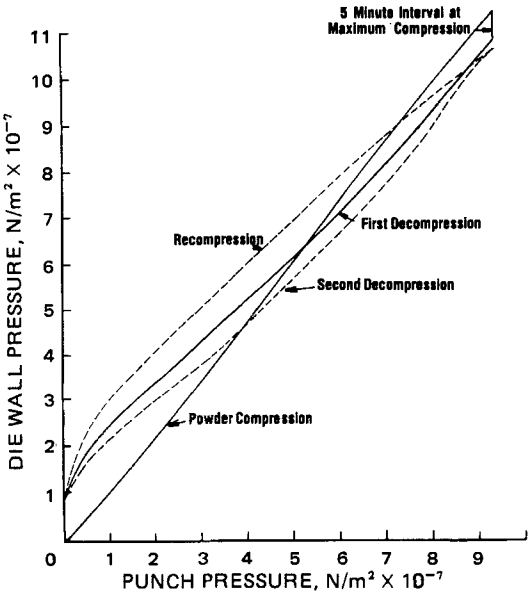

Figure 6—*Sitosterols: local die wall pressure* versus *mean punch pressure for compression–decompression cycles.*

The authors hope to equip the apparatus with a distance-measuring sensor so that the work of recompression and decompression may be determined. Certainly, the loop in Fig. 2 suggests that the work of recompression is much greater than the work done on the punch during decompression. Without a distance or volume measurement, the calculations cannot be made.

Figures 6–13 show similar results for sitosterols, spray-dried lactose, erythromycin, and sodium chloride. While differences in the detailed shapes of the curves are apparent, the general characteristics remain the same. Apparently, the previous discussion for sucrose applies equally to these materials.

Localized plastic deformation may occur at lower stresses than would be required to produce gross shear across the compact. The local shear stresses exceed the shear strength because of stress concentrations that occur around imperfections such as pores and density gradients. These internal local regions of shear may account for the apparently anelastic behavior in the recompression–decompression cycle. If localized shear occurs, the recompression–decompression cycle might not be completely reproducible, since there is no reason to expect the shapes of the stress concentrator regions that flow plastically during compression to be reconstructed in the decompression stage. Thus, it is not surprising that the observed maximum die wall pressure is less after each recompression (Fig. 2). This direction of change would be expected, since the die wall

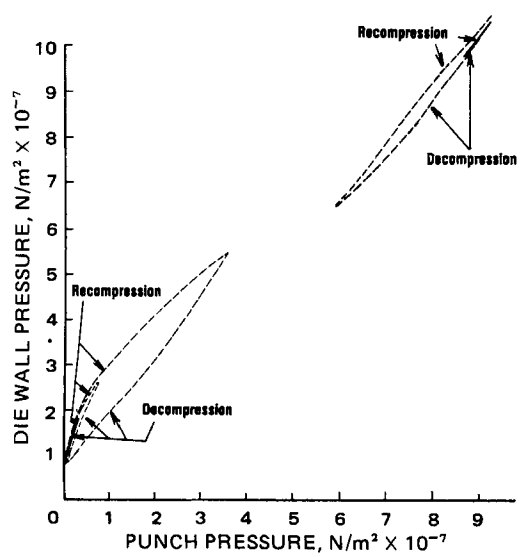

Figure 7—*Sitosterols: partial recompression–decompression cycles of a compact.*

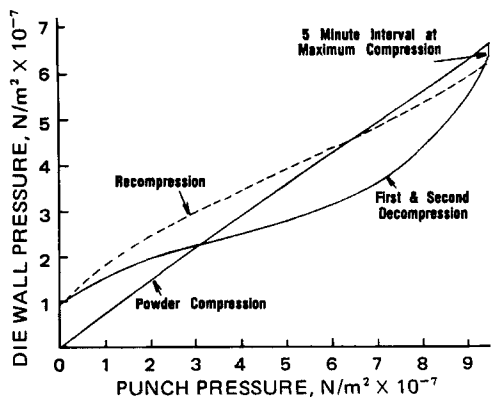

Figure 8—*Spray-dried lactose USP (hydrous): local die wall pressure* versus *mean punch pressure for compression–decompression cycles.*

pressure decreased during stress relaxation under constant punch pressure. The combined evidence of these observations and the time-dependent stress redistribution reported in Figs. 1, 2, and 14[10] strongly indicates the conclusion that local plastic deformation occurs in compacts.

Table I shows tensile strength values for compacts subjected to recompression–decompression cycling. The increase in strength that occurred with these materials is interpreted as an increase in true contact area between particles. Shear under a compressive load could produce an increased contact area. However, shear also may induce fracture, especially during decompression. Since the two processes produce opposite effects on the strength, not all materials will show the same trend. Most plastic materials, such as those used for the data in Table I, show increased strength. Figure 15 illustrates the case where the stresses during decompression led to fracture on the first decompression. Obviously, tensile strengths could not be determined. Phenacetin, methenamine, and acetaminophen, materials known to induce capping, show this kind of fracture. Apparently, these materials do not adequately relieve local stresses by plastic deformation; hence, fracture in shear occurs across the entire compact. For these materials, recompression curves are meaningless.

Brittle Fracture—The Griffith crack theory teaches that, for crack growth to occur, the energy stored at the tip of a crack must just exceed the energy required to form the two new surfaces resulting from the propagation of the crack. Also, the amount of energy stored at the tip of a crack is a function of the dimensions of the crack. An elementary description of the critical condition for crack growth is given by:

$$\sigma_c = K\sqrt{\frac{\gamma E}{L}} \qquad \text{(Eq. 10)}$$

where σ_c is the critical tensile stress for crack growth, γ is the surface energy, E is Young's modulus of elasticity, L is one-half the crack length, and K is a constant. In deriving this equation, the radius of curvature at the tip of the crack was assumed to be of molecular dimensions. The radius does not appear in Eq. 10 because it cancels against the same radius term, which occurs in the expression for the applicable stress concentration factor.

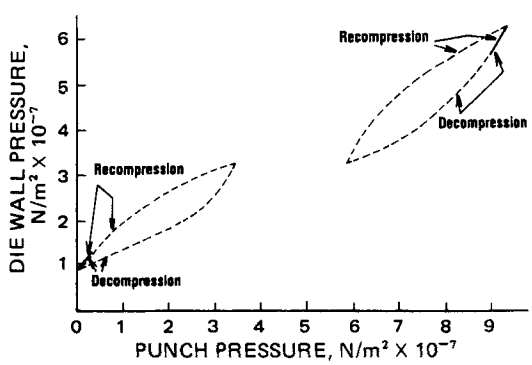

Figure 9—*Spray-dried lactose USP (hydrous): partial recompression–decompression cycles of a compact.*

[10] Figure 14 is basically a stress relaxation determination using the Milosovich apparatus (3) to obtain the data.

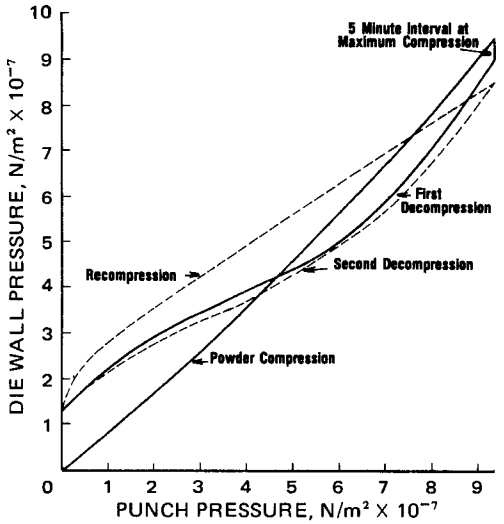

Figure 10—*Erythromycin USP: local die wall pressure* versus *mean punch pressure for compression–recompression cycles.*

The extent of the stress concentration, the stress concentration factor f, is a multiplier applied to the magnitude of the uniform stress calculated as if no flaw were present. A simple case may be used to illustrate stress concentration. If a slab is subjected to only a uniform tensile stress and the slab contains an elliptical hole with the long axis normal to the direction of the tensile stress, the tensile stress at the edge of the hole, as long as the hole is much smaller than the width of the slab, is given by:

$$f = 1 + 2\sqrt{\frac{L}{R}} \qquad \text{(Eq. 11)}$$

where L is one-half the length of the hole, and R is the radius of curvature of the tip of the hole.

Note that Eq. 11 reduces to a stress concentration factor of 3 for a round hole, regardless of its radius (its size still must be very much less than the slab size). When a second uniform stress is applied to the slab normal to the direction of the tensile stress, the stress concentration factor around a hole is not exactly 3. Figure 16 shows the stress concentration factor at a hole for various stress conditions (15).

The stress concentration concept is useful in understanding why ejection from a die can cause a compact to laminate. Theoretically, the radius of curvature at the edge of the die could be of molecular dimensions. Therefore, the stress concentration factor to be applied to the die wall pressure when a compact is partially ejected could be a very large number. Figure 17 is a photograph of an erythromycin compact that split off many layers as it was slowly ejected. The assumed mechanism is that a crack initiated at the edge and propagated across the compact. Materials that exhibit a high shear strength and, therefore, a high residual die wall pressure and also have a high propensity for brittle fracture may undergo

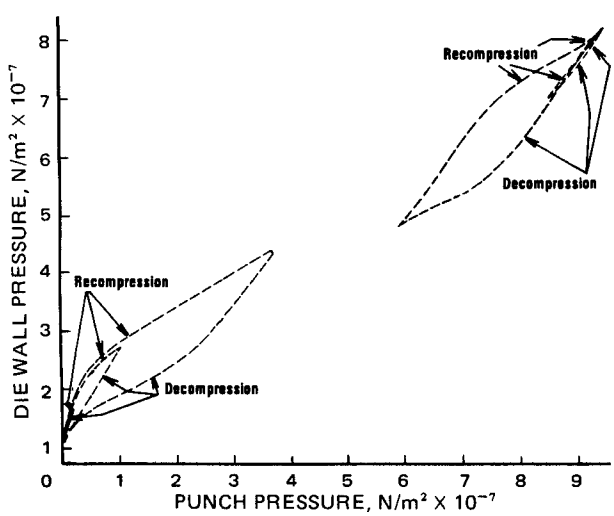

Figure 11—*Erythromycin USP: partial recompression–decompression cycles of a compact.*

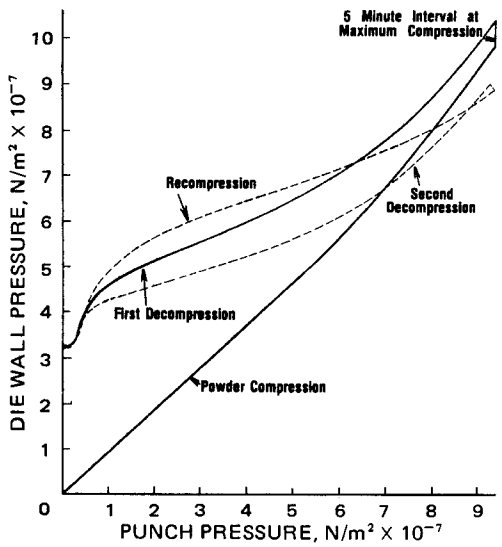

Figure 12—*Sodium chloride: local die wall pressure* versus *mean punch pressure for compression–decompression cycles different from other materials. The die wall pressure increased during the 5-min interval the maximum punch pressure was held constant.*

brittle fracture from points of very high stress concentration such as the die edge.

It should be possible to use the knowledge of stress relief at sites of stress concentration to characterize the tendency of compacts to propagate cracks. Suppose that a round hole is placed in the center of a compact and that it is subjected to a tensile stress. Tensile fracture might be expected to occur at exactly one-third of the tentile stress required to produce tensile fracture when no hole is present. However, this would be true only if the compact did not relieve the locally concentrated stresses at the edge of the hole by plastic deformation. If all excess stresses at the hole's edge were relieved, no observable differences in the tensile fracture force would be observed. Real materials should fracture at some intermediate value, the magnitude depending on their ability to relieve localized stresses. Since fracture by crack propagation from a flaw that concentrates stress is called brittle fracture, comparison of the strength with and without a hole has been used to define a parameter called the brittle fracture propensity (BFP). The BFP is calculated by:

$$\text{BFP} = 1/2\left[\frac{\sigma_T}{\sigma_{TO}} - 1\right] \qquad \text{(Eq. 12)}$$

where σ_T is the tensile strength without a hole, and σ_{TO} is the apparent tensile strength with a hole present.

The subtraction of one and division by two normalize the values of BFP so that the theoretical value range is 0–1 when the stress concentration factor is 3. Since the BFP value is an inverse measure of localized stress relief, it should indicate the tendency of a compact to laminate or cap.

A technique for measuring the BFP of compacts is based on the transverse compression of squares (2). Earlier work showed that if a

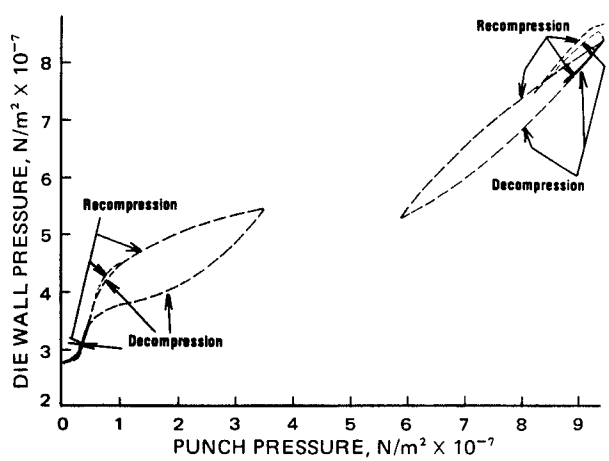

Figure 13—*Sodium chloride: partial recompression–decompression cycles of a compact.*

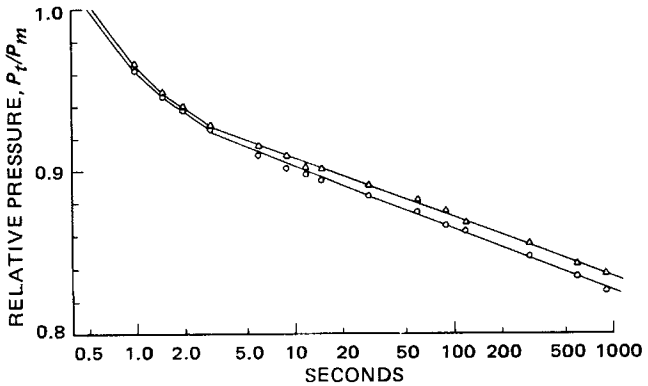

Figure 14—*Microcrystalline cellulose: relative punch pressure* versus *log time;* P_t *is pressure at time* t, P_m *is the maximum pressure applied, zero time corresponds to the start of the stress application, circles are data for an in air measurement, and triangles are data for an* in vacuo *measurement. Escape of air following compression did not alter the general shape of the curve. Maximum pressures applied were* 7.24×10^7 N/m^2 *in air and* 6.89×10^7 N/m^2 in vacuo; *slope values varied slightly with the maximum applied compression pressure and were usually steeper with an increase in the maximum pressure.*

square compact is centered on edge between two platens whose width is four-tenths of the width of the compact, the central region of the compact is under a nearly uniform shear stress (16). Figure 18 shows the fringe patterns obtained with polarized light through a transparent model substance, poly(methyl methacrylate). (Photoelastic methods of determining stress distributions use more sophisticated techniques to obtain and evaluate fringe patterns.) Comparison of the two fringe patterns clearly shows that when the hole is present, the magnitude of the stresses is changed markedly. Although isochromatic fringe lines are isoshear stress lines, one cannot determine the principal stresses without additional information. The techniques of photoelasticity are outside the scope of this discussion but do indeed permit the determination of stress concentration factors such as those shown in Fig. 16.

The stress condition at the center of a square compact in transverse compression is not simple tension. A compression stress is present in the direction normal to the tensile stress. Therefore, from the data displayed in Fig. 16 and from the analysis of Berenbaum and Brodie (16), which show that the ratio of tension to compression is approximately 0.28, it is evident that the stress concentration factor is approximately 3.25. The use of Eq. 12 with this method of tensile strength measurement will not limit the BFP values to less than unity, at least in theory, since the equation was normalized for a stress concentration factor of 3. In practice, one probably cannot make an intact compact of a material with a BFP of 1. Therefore, the observed range of values may not exceed the 0–1 range.

While it might be preferable to base the BFP on an exact theoretical analysis, one must recognize that the heterogeneous relative densities of a compact make a high level of precision most difficult to attain. Furthermore, difficulties not yet understood arise with this test. Therefore, the authors elected to use Eq. 12 to estimate the BFP, even when the evaluation of tensile strengths was made by the transverse compression of squares[11]. Added specifications should include the relative density of the compact because very soft compacts do not yield useful data. Nevertheless, sufficient accuracy exists for useful relative values to be obtained simply by adopting a standard procedure. Of course, compacts containing other flaws such as laminations will yield false values. When one observes a stepped fracture plane, one should suspect lamination and reject the data. If various laboratories were to attempt to obtain identical values for the BFP, very detailed specifications would be needed for high levels of precision.

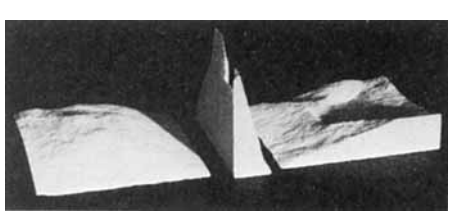

Figure 15—*Phenacetin compact that fractured in the die without ejection. Similar fracture occurs with acetaminophen and with some mixtures of these materials with excipients.*

[11] In the authors' studies, the platen width was 0.4 the tablet width, pads were used on the platens, and the hole diameter was 1.09 mm in a 38.1-mm square compact.

Table I—Tensile Strength of Compacts Subject to Various Compression Procedures

Material	Number of Compressions	Tensile[a] Strength, $N/m^2 \times 10^{-6}$	Significant[b] Difference, p
Aspirin	1	1.10	] <0.001
	4	1.26	
Sucrose	1	1.32	] 0.18
	4	1.37	
Lactose (spray dried)	1	1.45	] 0.08
	4	1.50	

[a] Average of five compacts. Maximum compression of 9.50×10^7 N/m^2. [b] Strengths are significantly different at listed p values. Brackets indicate the pair of values compared to obtain p value.

Experimental values for a few materials are listed in Table II. Materials known to induce capping have relatively large BFP values, as expected. The punch used to form compacts with a hole in the center is shown in Fig. 19.

Stress Relaxation—So far, the discussion has ignored an important variable—*viz.*, time. Plastic deformation is a time-dependent phenomenon. Shlanta and Milosovich (3) showed that compression stresses are relieved with time. Their experiments were similar to a relaxation study, since the size of the compact was fixed and the change in punch pressure with time was recorded. The authors used the Milosovich apparatus and confirmed the basic observation. Furthermore, every material examined by the authors with this apparatus underwent relaxation of the punch pressure (Figs. 14, 20, and 21). Because the compact is not under uniaxial compression during the stress relaxation, the quantitative interpretation of the experimental results is complicated. Furthermore, the slope is a function of the porosity of the compact. However, for the examples shown, the rank order is obvious. Materials that are known to cap exhibit slower stress relaxation.

The change of slope at the short time intervals observed in these stress *versus* log time plots suggests that some initially prominent mechanism soon becomes negligible. Because air entrapment has been propounded as the cause of lamination and capping, it was of interest to establish whether the diffusion of air from the compact was an initially prominent mechanism. Therefore, the stress relaxation experiments were repeated but with the powders in an evacuated die[12]. In no case were the general characteristics of the stress relaxation curves altered. Apparently, the air must escape in less than 0.4–0.7 sec from these materials (Figs. 14, 20, and 21). An apparatus that reduces the compression time to very small values is needed to explore this point further.

The relaxation of die wall pressure was discussed previously. Obviously, pressures at all points in a compact may not be undergoing stress relaxation identically. As indicated previously, the pressure at the center of the punch was increasing while the die wall pressure decreased (Fig. 1).

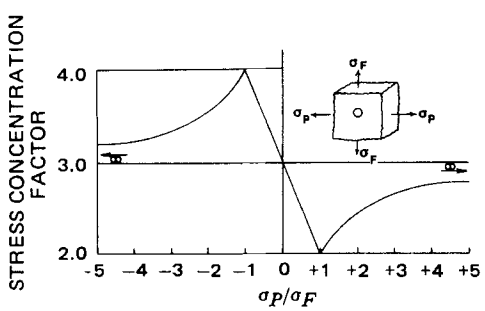

Figure 16—*Tensile stress concentration factor at the edge of a hole for biaxial stress conditions;* σ_P *and* σ_F *are stresses acting at right angles to each other. A negative value arises for* σ_P/σ_F *when one stress is compression and the other is tension. Hole diameter is much much smaller than dimensions in direction of stress. (Data from Ref. 12.)*

[12] Evacuable die 186-0002, Perkin-Elmer Corp., Norwalk, Conn.

Table II—Deformation and Fracture Properties of Pure Materials

Material	BFP[a]	P/σ_t[b]	E_e/E_p[c]
Methenamine	0.83	58	0.134
Erythromycin base	0.65	25	3.56
Ibuprofen	0.40	87	0.145
Sucrose	0.35	102	0.590
Starch, modified[d]	0.27	78	1.07
Lactose (spray dried)	0.18	193	0.844
Microcrystalline cellulose	0.04	25	1.45

[a] Brittle fracture propensity. All compacts were compressed at 9.5×10^7 N/m². [b] Mean deformation pressure divided by the tensile strength. All compacts had a relative density of 0.85. [c] Relative deformation energies (elastic/plastic) for deformation beneath a steel sphere; $E_e + E_p$ was the same for all materials. The relative density of all compacts was 0.85. [d] StaRx.

However, mean pressures may be decreasing if the compact increases its relative density as a result of stress relaxation, *i.e.*, as a function of time. Therefore, there is no reason to conclude that the two apparatuses yield conflicting results.

The evidence clearly indicates the existence in compacts of time-dependent properties of plastic deformation and stress relief. Therefore, the incidence of fracture also should be time dependent. Intact compacts of some pure medicaments, *e.g.*, acetaminophen, methenamine, and erythromycin, were made when the decompression was extended over several hours, even though rapid decompression produced fractured compacts.

Differences in the slopes of the initial segments of these plots should reflect the ability of the material to relieve stresses in a tableting machine. As expected, the stresses in methenamine decayed very slowly while those in sitosterols decayed much more rapidly. Stresses in erythromycin decayed much more rapidly than might be expected since they produced laminated compacts. This finding may account for the ability of erythromycin to withstand (not fracture) decompression but to fracture upon ejection where the time interval for decay of stress is very short.

Indentation Hardness—If a sphere is pressed against a compact surface hard enough to produce plastic flow beneath it, the mean pressure over the sphere–compact interface is essentially a constant when the chordal radius of the dent is much less than the radius of the sphere. This mean deformation pressure[13], P, is a measure of the hardness of the compact. The yield value for plastic flow is approximately 0.36 P.

The role of plastic flow in determining residual die wall pressure and in relieving concentrated stresses was emphasized in the preceding discussion. Therefore, the determination of P should be of direct interest. A method based on the rebound of a steel sphere from a compact was used (4). For comparison, the values of P for compacts with a relative density, ρ_r, of 0.85 were used for all materials. Plots of log P *versus* ρ_r are nearly straight lines and were used in interpolation to obtain the 0.85 relative density value.

Perhaps the ratio of the deformation pressure, P, divided by the tensile strength is of more interest than the deformation pressure alone. If both shear strength and tensile strength arise from the same bonded areas in a given compact, then the ratio P/σ_T for materials should have similar values unless the mechanical structure of the compact influences disproportionally the magnitude of these terms. The magnitude of P should not be influenced by crack propagation, but that of σ_T should be. Thus, if the ratio of P to σ_T varies over a large range, the pore structure may be affecting the tensile strength values. Crack propagation occurs

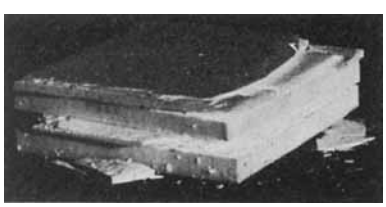

Figure 17—*Erythromycin base compact that fractured when ejected from the die. Starch and methenamine compacts fractured in a similar manner.*

[13] Analogous to P in Eq. 1, except that Eq. 1 was measured at contact points between particles. Here, the mean pressure is over a macroscopic area that may contain pores. Nevertheless, the equations for nonporous materials may be used (4).

Table III—Influence of Machine Speed and Precompression Force on the Final Compression Force that Produced Fractured Tablets[a]

Machine Speed, rpm	Precompression Force, Metric Tons	Final Compression Force, Metric Tons	
		No Lamination	Lamination
	Cupped Punches[b]		
44	0	0.907	1.134
	0.225	1.361	1.814
	0.454	1.814	1.905
32	0	1.270	1.361
	0.225	1.814	1.905
	0.454	1.905	2.041
24	0	1.588	1.814
	0.225	2.268	2.495
	0.454	2.268	2.495
	Flat Punches[c]		
37	0	1.361	2.268

[a] See footnote 6 in text for the composition of the formulas. [b] When 11.9-mm flat punches and die were used with the same formulation, no lamination was observed. [c] Very little work was done with the flat punches because a formula that produced a good bond at lower pressures and laminated at the highest pressures was not developed.

when the tensile stresses at a flaw exceed the tensile strength without the shear stresses exceeding the shear strength, *i.e.*, without stress relief occurring by plastic flow. Thus, the ratio of P/σ_T might correlate with the BFP. If true, a relatively large value of P/σ_T should indicate an increased propensity for brittle fracture. Factors that could affect this comparison are differences in the surface energy of the solid, the modulus of elasticity of the compact, and the internal flaw structure that concentrates stresses. Table II shows the results of these measurements.

It is obvious from Table II that the P/σ_T values do not correlate with the BFP values. Nor do the P/σ_T values correlate with the tendency to form fractured tablets. It seems more reasonable to conclude that both σ_T and P are measuring different manifestations of the strength of the true contact areas without gross effects from stress concentration at pores controlling the values.

The impact–rebound method of determining P provides measurements of both the energy used in the permanent deformation and the energy of the elastic recovery from the impact. A high energy of elastic deformation per unit of plastic deformation energy, E_e/E_p, could indicate that large elastic stresses develop within the compact. Thus, it is of interest to compare the magnitude of E_e/E_p for the various materials. The last column of Table II lists the experimental values for several materials. Obviously, the magnitudes of the ratios of E_e/E_p do not correlate with the brittle fracture properties of the compact.

Tablet Making—Stress relaxation is believed to explain some practical problems encountered in tableting. When lamination is a problem and the production volume of a rotary machine is needed, a machine that provides precompression should be selected. The precompressed compact has time to undergo some stress relaxation before the final compression is applied. To maximize the stress relaxation, the precompression pressure should be near the maximum that will not by itself introduce lamination. This will maximize the stress relaxation that can occur before the final compression. A long dwell time under compression also will increase the time for stress relaxation. Thus, a slow operating speed also increases the time available for stress relaxation. The final compression should use as small a force as possible to obtain an acceptable tablet, since there is less stress acting at a smaller compression force to cause the compact to fracture. If the BFP of the formulation is not too high, one should be able to make a satisfactory product under the conditions described.

The use of deep oval punches is known to engender capping. Obviously, a large quantity of material in the "dome" is expanding radially as the punch is removed. Since the main body of the tablet cannot expand radially into the die wall, large shear stresses develop. Flat punches avoid this contribution to the shear stress. Therefore, when possible, tablet shape selection should be made to reduce stress gradients during tableting.

Other studies have demonstrated the effects of precompression[14]. They were repeated in the present study to observe the effects of precom-

[14] A. C. Shah, The Upjohn Co., unpublished data.

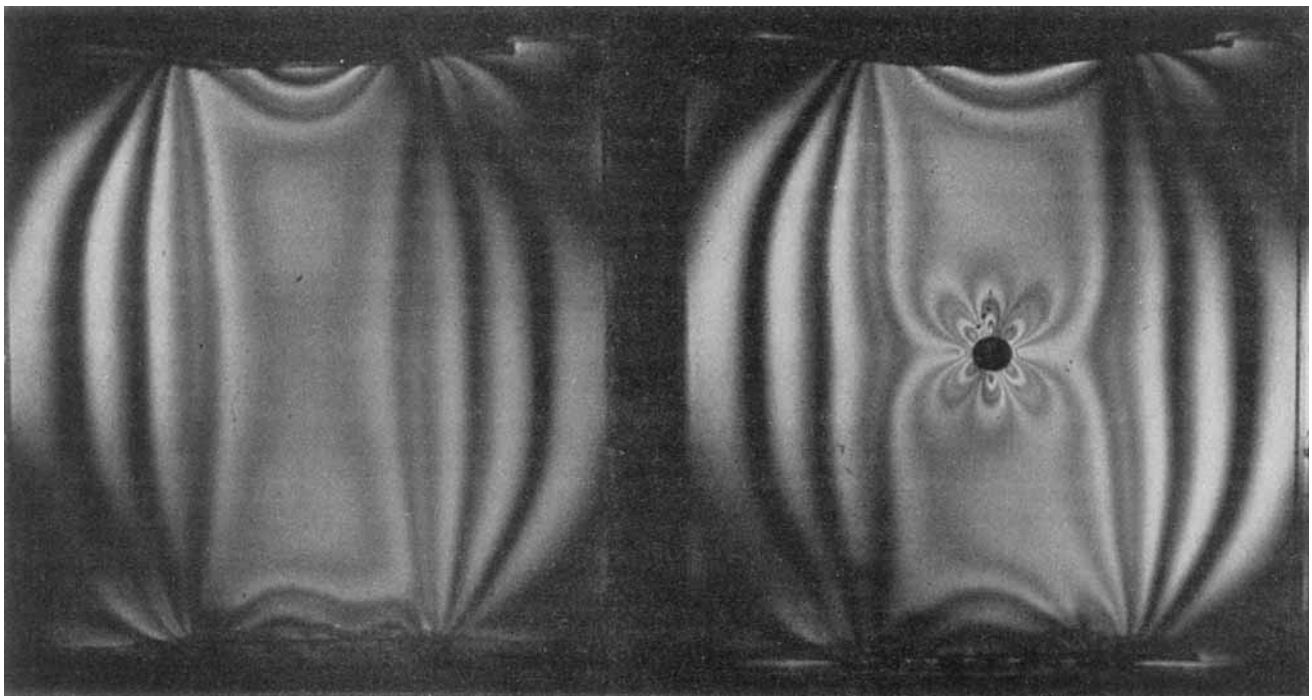

Figure 18—*Examples of simple fringe patterns obtained with and without a hole in a compact subjected to transverse compression. These photographs were made with white light and simple polarizers and are not suitable for stress analysis use. However, they identify high stress gradient areas.*

pression on final compression, the influence of machine speed, and the influence of punch shape (Table III). The theory predicts the pattern of the experimental results. Of course, quantitative predictions are not possible with the present knowledge. The minimum precompression force for intact compacts was a function of machine speed, final compression force, and punch shape. Conversely, the maximum final compression force that produced intact compacts was a function of the precompression force, the machine speed, and the punch shape. Conditions that increased the amount of stress relaxation permitted increased compression force and vice versa.

If even the best conditions of tableting still produce laminated tablets, reformulation is necessary. One should then seek an excipient material that has a very low BFP value to add to the high BFP medicament. Of course, in practice, one must also consider effects on disintegration, *etc.* Nevertheless, an understanding of the discussed principles provides much guidance in the formulation of the compressed tablet dosage form.

SUMMARY

Under the nonisostatic compression force of tableting, the powder particles undergo sufficient plastic deformation to produce a die wall pressure in excess of that that can be relieved by the elastic recovery accompanying the removal of the punch pressure. This die wall pressure produces internal stress sufficiently high to cause internal shear in the compact during the decompression. Plastic deformation occurs in repeated recompression and decompression cycles. In some materials, the internal shear stresses cause a crack to propagate and fragmentation occurs. If the stresses during decompression are not sufficient to produce crack propagation within the die during decompression, the stress concentrations developed at the edge of the die may produce crack propagation (lamination) as the tablet is ejected.

Since shear stresses develop during decompression and/or ejection, the failure to fracture appears to be due to the ability of a material to relieve shear stresses by localized shear flow, *i.e.*, plastic deformation. This property can be measured by comparing the tensile strength of a compact that contains a built-in stress concentrator "defect" with one that does not. By using this knowledge, a test was designed that indicates a property of a material called the "brittle fracture propensity." The brittle fracture propensity value indicates whether or not capping or lamination may be a problem in tableting the material.

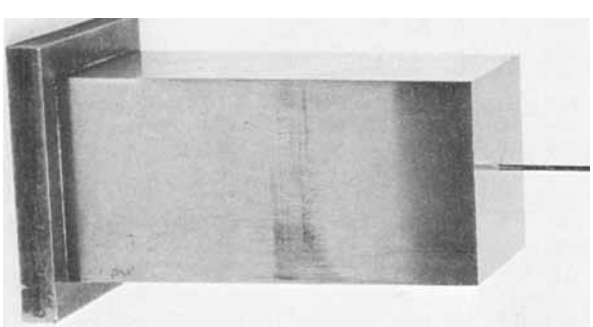

Figure 19—*Special punch used to make compacts with small hole in center. Pin is spring loaded and retractable so that any reasonable compact thickness can be used.*

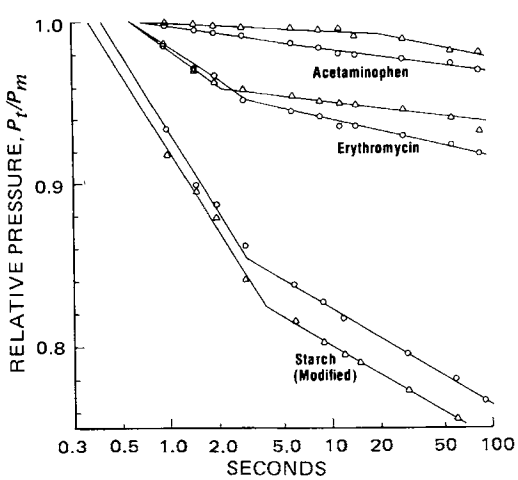

Figure 20—*Relative punch pressure* versus *log time. Zero time corresponds to the start of the stress application. Circles are data from an in air measurement; triangles are data from an* in vacuo *measurement. Material with the slowest rate of relaxation fractured upon decompression in the die; erythromycin laminated upon ejection. Maximum pressures (in* $N/m^2 \times 10^{-7}$*) were: acetaminophen, air 7.31 and* in vacuo *7.03; erythromycin, air 7.86 and* in vacuo *8.89; and modified starch, air 6.62 and* in vacuo *5.31.*

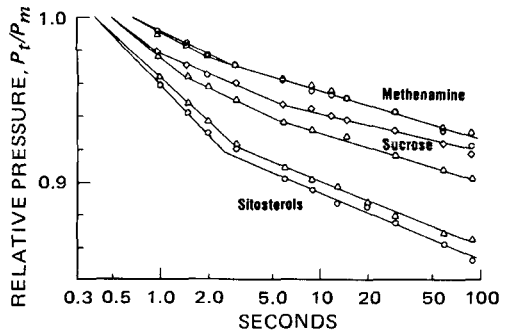

Figure 21—*Relative punch pressure* versus *log time. Zero time corresponds to the start of stress application. Circles and diamonds are data from an in air measurement; triangles are data from an* in vacuo *measurement. Only material with the slowest rate of relaxation fractured upon rapid decompression in the die. Maximum pressures (in* $N/m^2 \times 10^{-7}$*) were: methenamine, air 8.34 and* in vacuo *8.41; sucrose, air 6.96 and* in vacuo *6.52; and sitosterols, air 4.62 and* in vacuo *4.07.*

The time-dependent nature of plastic flow or stress relaxation also must be considered and may account for differences in the properties of tablets produced on various machines or at various machine settings.

REFERENCES

(1) E. L. Knoechel, C. C. Sperry, H. E. Ross, and C. J. Linter, *J. Pharm. Sci.*, **56**, 109 (1967).

(2) E. N. Hiestand and C. B. Peot, *ibid.*, **63**, 605 (1974).

(3) S. Shlanta and G. Milosovich, *ibid.*, **53**, 562 (1964).

(4) E. N. Hiestand, J. M. Bane, Jr., and E. P. Strzelinski, *ibid.*, **60**, 758 (1971).

(5) A. S. Rankell and T. Higuchi, *ibid.*, **57**, 574 (1968).

(6) P. York and N. Pilpel, *J. Pharm. Pharmacol.*, **25**, S-1P (1973).

(7) E. N. Hiestand, *Pharm. Ind.*, **34**, 262 (1972).

(8) P. Dyachenko, N. Tolkacheva, G. Andrew, and T. Karpova, "The Actual Contact Area Between Touching Surfaces," Consultants Bureau, New York, N.Y., 1964.

(9) F. C. Yip and J. E. S. Venart, *J. Phys. D., Appl. Phys.*, **4**, 1470 (1971).

(10) D. Train, *J. Pharm. Pharmacol.*, **8**, 745 (1956).

(11) E. Shotton and J. A. Hersey, in "Theory and Practice of Industrial Pharmacy," L. Lachman, H. Lieberman, and J. Kanig, Eds., Lea & Febiger, Philadelphia, Pa., 1970, chap. 9.

(12) E. Nelson, *J. Am. Pharm. Assoc., Sci. Ed.*, **44**, 494 (1955).

(13) S. Leigh, J. E. Carless, and B. W. Burt, *J. Pharm. Sci.*, **56**, 888 (1967).

(14) J. E. Carless and S. Leigh, *J. Pharm. Pharmacol.*, **26**, 289 (1973).

(15) C. Lipson and R. C. Juvinall, "Handbook of Stress and Strength," Macmillan, New York, N.Y., 1963.

(16) R. Berenbaum and I. Brodie, *Br. J. Appl. Phys.*, **10**, 281 (1959).

ACKNOWLEDGMENTS AND ADDRESSES

Received December 4, 1975, from *Pharmacy Research, The Upjohn Company, Kalamazoo, MI 49001.*

Accepted for publication June 8, 1976.

The authors thank the many people that assisted in various ways with this research. Mr. H. Ballen and Mr. C. C. Sperry designed the special apparatuses used. Dr. G. Milosovich and the University of Michigan School of Pharmacy loaned the stress relaxation apparatus. Mr. L. H. Macdonald and Mr. J. F. Glasscock worked with the phenacetin formulations.

[x] To whom inquiries should be directed.

Solubility Studies of Silver Sulfadiazine

R. U. NESBITT, Jr. *, and B. J. SANDMANN [x]

Abstract □ The solubility of silver sulfadiazine as a function of pH was determined in nitric acid–potassium nitrate buffer for pH 2–3 and in 2-(*N*-morpholino)ethanesulfonic acid buffer for pH 6–7. As the salt of a weak organic acid, silver sulfadiazine exhibits the anticipated increase in solubility with an increasing hydrogen-ion concentration. Measurement of the silver-ion concentration was carried out using a silver-ion selective electrode. The methods of known subtraction and known addition were utilized to measure the total concentration of the silver ion in solution. Evidence was obtained to indicate that the salt is completely ionized in aqueous solution.

Keyphrases □ Silver sulfadiazine—solubility as a function of pH, potentiometric study □ Solubility—silver sulfadiazine as a function of pH, potentiometric study □ pH—effect on solubility of silver sulfadiazine, potentiometric study □ Potentiometry—study of solubility of silver sulfadiazine as a function of pH □ Anti-infectives, topical—silver sulfadiazine, solubility as a function of pH, potentiometric study

Silver sulfadiazine, a substance with extremely low water solubility, was reported to be particularly efficacious as a topical antibacterial agent for the control of *Pseudomonas* infection in burns (1). When applied locally to burned skin, silver sulfadiazine is claimed to offer definite therapeutic advantages over other similar chemotherapeutic agents used to treat infection. Unlike other drugs that diffuse rapidly or deplete chloride ions from body fluids, silver sulfadiazine remains in the wound exudate for a prolonged effect and appears to enhance conditions favorable for epithelial regeneration.

BACKGROUND

The mode of antibacterial action is different than that of sulfonamides, because the drug is not antagonized *in vitro* by aminobenzoic acid. In binding studies using radioactive silver sulfadiazine prepared from radioactive ^{110}Ag- and ^{35}S-tracers, the silver ion was found to bind with the *Pseudomonas* cells. No cellular binding of sulfadiazine was detected (2, 3).

The binding of silver to bacterial DNA was proposed as important for inhibiting microbial growth. Silver displaces the hydrogen bonds between adjacent nitrogens of the purines (adenine or guanine) and pyrimidines (thymine and cytosine) in the DNA molecule. The nitrogen–silver bonds, once formed, appear to be stronger than the nitrogen–hydrogen bonds; therefore, bacteria having this silver–nucleic acid complex presumably